

# Agonist-, Antagonist-, and Benzodiazepine-Induced Structural Changes in the $\alpha_1$ Met<sup>113</sup>-Leu<sup>132</sup> Region of the GABA<sub>A</sub> Receptor

Jessica Holden Kloda<sup>1</sup> and Cynthia Czajkowski

Department of Physiology and Molecular and Cellular Pharmacology Program, University of Wisconsin-Madison, Madison, Wisconsin

Received July 7, 2006; accepted November 15, 2006

## ABSTRACT

The structural basis by which agonists, antagonists, and allosteric modulators exert their distinct actions on ligand-gated ion channels is poorly understood. We used the substituted cysteine accessibility method to probe the structure of the GABA<sub>A</sub> receptor in the presence of ligands that elicit different pharmacological effects. Residues in the  $\alpha_1$ Met<sup>113</sup>-Leu<sup>132</sup> region of the GABA binding site were individually mutated to cysteine and expressed with wild-type  $\beta_2$  and  $\gamma_2$  subunits in *Xenopus laevis* oocytes. Using electrophysiology, we determined the rates of reaction of *N*-biotinaminoethyl methanethiosulfonate (MTSEA-biotin) with the introduced cysteines in the resting (unliganded) state and compared them with rates determined in the presence of GABA (agonist), 4-[6-imino-3-(4-methoxyphenyl)pyridazin-1-yl]butanoic acid hydrobromide (SR-95531; antagonist), pentobarbital (allosteric modulator), and flurazepam (allosteric modulator).  $\alpha_1$ N115C,  $\alpha_1$ L117C,

$\alpha_1$ T129C, and  $\alpha_1$ R131C are predicted to line the GABA binding pocket because MTSEA-biotin modification of these residues decreased the amount of current elicited by GABA, and the rates/extents of modification were decreased both by GABA and SR-95531. Reaction rates of some substituted cysteines were different depending on the ligand, indicating that barbiturate- and GABA-induced channel gating, antagonist binding, and benzodiazepine modulation induce specific structural rearrangements. Chemical reactivity of  $\alpha_1$ E122C was decreased by either GABA or pentobarbital but was unaltered by SR-95531 binding, whereas  $\alpha_1$ L127C reactivity was decreased by agonist and antagonist binding but not affected by pentobarbital. Furthermore,  $\alpha_1$ E122C,  $\alpha_1$ L127C, and  $\alpha_1$ R131C changed accessibility in response to flurazepam, providing structural evidence that residues in and near the GABA binding site move in response to benzodiazepine modulation.

GABA<sub>A</sub> receptors are ligand-gated ion channels (LGICs) that mediate fast inhibitory synaptic neurotransmission in the brain and are allosterically modulated by a variety of compounds, including benzodiazepines (BZDs), barbiturates, anesthetics, and neuroactive steroids (Akabas, 2004). Identifying conformational movements that occur in the receptor in response to binding of these different classes of compounds is

critical for understanding the molecular mechanisms underlying their therapeutic actions. According to allosteric theory, modulators bind to a site on the protein that is distinct from the agonist binding site and exert their effects by initiating an allosteric transition in the protein that indirectly modifies the conformation of the binding site (Changeux and Edelstein, 1998). In this study, we used the substituted cysteine accessibility method to monitor the accessibility of residues in the  $\alpha_1$ Met<sup>113</sup>-Leu<sup>132</sup> region of the GABA binding site in the presence of GABAergic ligands that elicit distinct pharmacological effects. In particular, we were interested in determining whether BZD binding induces structural rearrangements in or near the GABA binding site. In addition, we were interested in investigating the mechanisms underlying how orthosteric agonist binding triggers channel opening and orthosteric antagonist binding does not.

The GABA<sub>A</sub> receptor belongs to the Cys-loop superfamily of LGICs, which includes the nicotinic acetylcholine (nACh),

This work was supported by a Pharmaceutical Research and Manufacturers of America Foundation Predoctoral Fellowship (to J.H.K.), National Institute of Neurological Disorders and Stroke grant NS34727 (to C.C.), and National Alliance for Research on Schizophrenia and Affective Disorder Award (to C.C.).

Portions of this work were previously presented at the Annual Meeting of the Society for Neuroscience 2001 in San Diego, CA and 2003 in New Orleans, LA.

<sup>1</sup> Current affiliation: Laboratory of Membrane Biochemistry & Biophysics, National Institute on Alcohol Abuse and Alcoholism, National Institutes of Health, Bethesda, Maryland.

Article, publication date, and citation information can be found at <http://molpharm.aspetjournals.org>.  
doi:10.1124/mol.106.028662.

**ABBREVIATIONS:** LGIC, ligand-gated ion channel; BZD, benzodiazepine; nACh, nicotinic acetylcholine; 5-HT<sub>3</sub>, serotonin-type-3; AChBP, acetylcholine binding protein; SR-95531, 4-[6-imino-3-(4-methoxyphenyl)pyridazin-1-yl]butanoic acid hydrobromide; MTSES, methanethiosulfonate ethylsulfonate; MTSEA, methanethiosulfonate ethylammonium; LBD, ligand binding domain.

serotonin-type-3 (5-HT<sub>3</sub>), GABA<sub>C</sub>, and glycine receptors. Much is known about the structure of these receptors from the recent 4-Å resolution model of the nACh receptor (Unwin, 2005), the crystallographic structure of the related acetylcholine binding protein (AChBP) (Brejc et al., 2001; Celie et al., 2004) and decades of biochemical and electrophysiological studies (Akabas, 2004). For receptors in this superfamily, binding of neurotransmitter takes place at the extracellular N-terminal domain of the protein at the interface of two adjacent subunits and is coordinated by residues from at least six noncontiguous polypeptide regions, designated loops A to F, three in each subunit (Akabas, 2004).

The  $\alpha_1\beta_2\gamma_2$  GABA<sub>A</sub> receptor subtype ( $\beta:\alpha:\beta:\alpha:\gamma$  viewed counterclockwise from the synaptic cleft) is the most abundant in vivo (Sieghart and Sperk, 2002) and the two GABA binding sites are located at the interfaces between the  $\beta$  and  $\alpha$  subunits ( $\beta:\alpha$ ), with residues from each subunit contributing to the binding site (Sigel et al., 1992; Amin and Weiss, 1993; Smith and Olsen, 1994; Boileau et al., 1999; Westh-Hansen et al., 1999; Wagner and Czajkowski, 2001; Boileau et al., 2002; Holden and Czajkowski, 2002; Newell and Czajkowski, 2003; Newell et al., 2004). The BZD binding site is also located on the extracellular N-terminal domain of the receptor and is situated at the interface between the  $\alpha$  and  $\gamma$  subunits ( $\alpha:\gamma$ ) (Sigel, 2002). Although the structures of the GABA and BZD binding sites are relatively well known, the protein movements underlying GABA-induced channel activation and BZD-mediated receptor modulation are less well understood.

In the present study, we focused on the  $\alpha_1\text{Met}^{113}\text{-Leu}^{132}$  region of the GABA binding site (loop E, Fig. 1). Loop E of the GABA binding pocket is physically linked to the BZD binding site (loop A –  $\alpha_1\text{His}^{101}$ ) by a short stretch of 11 amino acid residues. We reasoned that if BZD binding triggered structural changes in the GABA binding site, then loop E was in a perfect position for potentially detecting these movements. In addition, residues in this region of the GABA binding site, besides directly contacting ligand, are likely to be important for mediating local movements in the site involved in coupling neurotransmitter binding to channel gating. Mutations of residues in the Loop E binding regions of the nACh and 5-HT<sub>3</sub> receptors have been shown to alter channel gating (Ohno et al., 1996; Venkataraman et al., 2002; and Beene et al., 2004).

In this study, we demonstrate that flurazepam binding to the GABA<sub>A</sub> receptor induces conformational rearrangements in the GABA binding site, providing structural evidence for reciprocal allosteric interactions between the GABA and BZD binding sites. We identify four residues,  $\alpha_1\text{Asn}^{115}$ ,  $\alpha_1\text{Leu}^{117}$ ,  $\alpha_1\text{Thr}^{129}$ , and  $\alpha_1\text{Arg}^{131}$ , that participate in forming part of the GABA binding site, and we present evidence that binding of GABA and the competitive antagonist SR-95531 trigger different local movements within the site, which are likely correlated with their different abilities in promoting channel opening.

## Materials and Methods

**Site-Directed Mutagenesis.** The  $\alpha_1$  cysteine mutants were engineered using recombinant polymerase chain reaction as described previously (Boileau et al., 1999; Kucken et al., 2000). Individual cysteine substitutions were made in the rat  $\alpha_1$  subunit at  $\text{Met}^{113}$ ,

$\text{Pro}^{114}$ ,  $\text{Asn}^{115}$ ,  $\text{Lys}^{116}$ ,  $\text{Leu}^{117}$ ,  $\text{Leu}^{118}$ ,  $\text{Arg}^{119}$ ,  $\text{Ile}^{120}$ ,  $\text{Thr}^{121}$ ,  $\text{Glu}^{122}$ ,  $\text{Asp}^{123}$ ,  $\text{Gly}^{124}$ ,  $\text{Thr}^{125}$ ,  $\text{Leu}^{126}$ ,  $\text{Leu}^{127}$ ,  $\text{Tyr}^{128}$ ,  $\text{Thr}^{129}$ ,  $\text{Met}^{130}$ ,  $\text{Arg}^{131}$ , and  $\text{Leu}^{132}$  where the numbering reflects the position in the mature  $\alpha_1$  subunit protein sequence. The cysteine mutants were subcloned into pGH19 for expression in *Xenopus laevis* oocytes as described previously (Boileau et al., 1998). The presence of the mutations was verified by restriction endonuclease digestion and double-strand cDNA sequencing.

**Expression in Oocytes.** *X. laevis* oocytes were prepared as described previously (Boileau et al., 1998). cRNA transcripts were generated using the mMessage T7 kit (Ambion, Austin, TX). GABA<sub>A</sub> receptor rat  $\alpha_1$  or  $\alpha_1$  mutants were expressed with wild-type rat  $\beta_2$  and  $\gamma_2$  subunits by injection of cRNA into oocytes (0.1 ng of  $\alpha$  and  $\beta$  subunits/oocyte and 1.4 ng of  $\gamma$  subunit/oocyte, except for  $\alpha_1\text{R119C}\beta_2\gamma_2$ , which was injected at 6:1:6 ng of  $\alpha_1/\beta_2/\gamma_2$ ).  $\alpha_1\text{R119C}$  was also expressed with the wild-type rat  $\beta_2$  subunit alone and injected at 10:1 ng of  $\alpha_1/\beta_2$  for some experiments, because higher receptor expression levels were achieved in the absence of the  $\gamma_2$  subunit. The oocytes were stored in ND96 medium (96 mM NaCl, 2 mM KCl, 1 mM MgCl<sub>2</sub>, 1.8 mM CaCl<sub>2</sub>, and 5 mM HEPES, pH 7.4) supplemented with 100  $\mu\text{g}/\text{ml}$  gentamicin and 100  $\mu\text{g}/\text{ml}$  bovine serum albumin for 2 to 14 days and used for electrophysiological recordings.

**Voltage-Clamp Analysis.** Oocytes under two-electrode voltage-clamp ( $V_{\text{hold}}$  of  $-80$  mV) were continuously perfused with ND96 at a rate of 5 ml/min. The bath volume was 200  $\mu\text{l}$ . GABA, SR-95531 (Sigma, St. Louis, MO), pentobarbital (Sigma/RBI, Natick, MA) and flurazepam (Sigma/RBI) were dissolved in ND96. Stock solutions of MTSEA-biotin (Biotium, Hayward, CA) were prepared in dimethyl sulfoxide (final concentration,  $\leq 2\%$ ). Standard two-electrode volt-

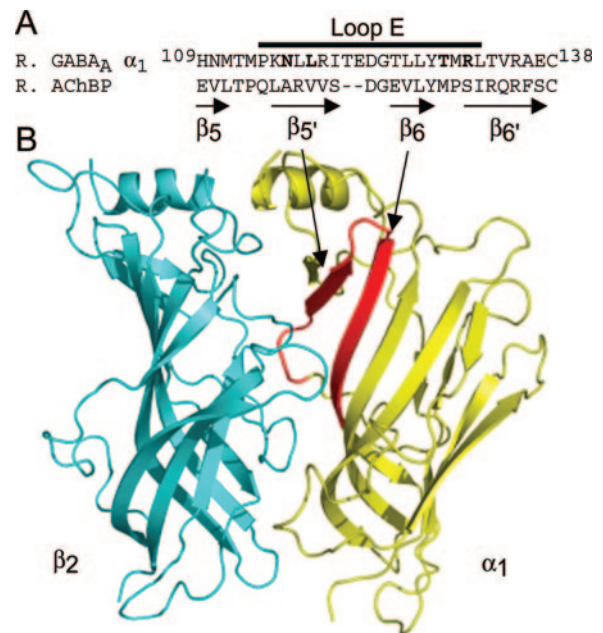


**Fig. 1.** The  $\alpha_1\text{Met}^{113}\text{-}\alpha_1\text{Leu}^{132}$  region of the GABA<sub>A</sub> receptor. A, alignment of the rat GABA<sub>A</sub> receptor  $\alpha_1\text{His}^{109}\text{-}\alpha_1\text{Cys}^{138}$  region with the analogous region of the AChBP (Brejc et al., 2001). The numbering corresponds to the position of the residues in the mature GABA<sub>A</sub> receptor  $\alpha_1$  subunit. The dashes indicate gaps in the amino acid sequence alignment. The residues in the GABA<sub>A</sub> receptor loop E region ( $\alpha_1\text{Met}^{113}\text{-}\alpha_1\text{Leu}^{132}$ ) that were mutated to cysteine are marked by a bar above the sequence. Residues identified in this study that line the core of the GABA binding site are bold. The arrows under the AChBP sequence denote  $\beta$ -strands determined in the crystal structure of AChBP. B, homology model of the extracellular N-terminal domains of the GABA<sub>A</sub> receptor  $\alpha_1$  and  $\beta_2$  subunits based on the crystal structure of the AChBP (Brejc et al., 2001) viewed from the side. The  $\beta_2$  subunit is shown in cyan and the  $\alpha_1$  subunit in yellow. The  $\alpha_1\text{Met}^{113}\text{-}\alpha_1\text{Leu}^{132}$  region ( $\beta$ -strands 5' and 6', loop E) is highlighted in red.

age-clamp recording was carried out using a GeneClamp 500 amplifier (Molecular Devices, Sunnyvale, CA) interfaced to a computer with a Digidata 1200 (Molecular Devices). Electrodes were filled with 3 M KCl and had resistances of 0.5 to 2.0 M $\Omega$  in ND96. Data acquisition was performed using pClamp 6 (Axon Instruments).

**EC<sub>50</sub> Analysis.** Concentration-response experiments were performed as described previously (Wagner and Czajkowski, 2001). In brief, these experiments used a low concentration of GABA (EC<sub>2</sub>-EC<sub>7</sub>) immediately before the test concentration of agonist to correct for any slow drift in GABA responses that might occur during the experiment. Currents elicited by each test concentration were normalized to the corresponding low-concentration current. Concentration-response data were fit to the following equation:  $I = I_{\max}/(1 + (EC_{50}/[A])^{n_H})$ , where  $I$  is the peak response to a given concentration of GABA,  $I_{\max}$  is the maximum amplitude of current,  $EC_{50}$  is the concentration of GABA that produces a half-maximal response,  $[A]$  is the concentration of GABA, and  $n_H$  is the Hill coefficient.

**IC<sub>50</sub> Analysis.** IC<sub>50</sub> values were measured as described previously (Wagner and Czajkowski, 2001). SR-95531 IC<sub>50</sub> values were measured by applying a fixed concentration of GABA (EC<sub>20</sub>-EC<sub>60</sub>) immediately followed by coapplication of the same concentration of GABA and a test concentration of SR-95531. Inhibition was calculated as  $I_{GABA + SR-95531}/I_{GABA}$ , where  $I_{GABA + SR-95531}$  is the current elicited in the presence of GABA and SR-95531, and  $I_{GABA}$  is the current elicited by GABA alone. Data were fit to the following equation: inhibition =  $1 - 1/(1 + (IC_{50}/[Ant])^{n_H})$ , where  $IC_{50}$  is the concentration of antagonist that blocks half of  $I_{GABA}$ ,  $[Ant]$  is the concentration of antagonist, and  $n_H$  is the Hill coefficient. Apparent  $K_I$  values were calculated using the Cheng-Prusoff/Chou equation (Cheng and Prusoff, 1973; Chou, 1974):  $K_I = IC_{50}/(1 + ([A]/EC_{50}))$ , where  $[A]$  is the concentration of GABA used and  $EC_{50}$  is the concentration of GABA that elicits a half-maximal response.

**Pulse Protocol for Measuring the Effect of MTSEA-Biotin on Introduced Cysteines.** GABA-elicited currents (EC<sub>40</sub>-EC<sub>60</sub>) were stabilized before application of MTSEA-biotin by applying GABA at 10-min intervals until the peak GABA-activated currents ( $I_{GABA}$ ) varied by <10%. The oocyte was allowed to recover for 3 min and treated with MTSEA-biotin (2 mM) and washed again for 5 min. GABA (EC<sub>40</sub>-EC<sub>60</sub>) was then reapplied. The effect of MTSEA-biotin was calculated as  $(I_{GABA-post}/I_{GABA-pre}) - 1$ , where  $I_{GABA-post}$  is the current elicited by GABA after MTSEA-biotin application, and  $I_{GABA-pre}$  is the current elicited by GABA before MTSEA-biotin application.

For  $\alpha_1$ M113C $\beta_2$  $\gamma_2$  and  $\alpha_1$ N115C $\beta_2$  $\gamma_2$ , the pulse protocol was modified to determine whether GABA or SR-95531 had any effect on the ability of MTSEA-biotin to inhibit  $I_{GABA}$ . In these experiments, GABA (EC<sub>40</sub>-EC<sub>60</sub>) was applied at 10-min intervals until the response stabilized. A high concentration of GABA or SR-95531 (EC<sub>90</sub>-EC<sub>100</sub>) was applied (2 min), and the cell was washed again (5 min). GABA (EC<sub>40</sub>-EC<sub>60</sub>) was then reapplied. The cell was stabilized until GABA-activated currents varied by <10%. High concentration GABA or SR-95531 was then applied in the presence of MTSEA-biotin (2 mM, 2 min). The cell was washed for 5 min and GABA (EC<sub>40</sub>-EC<sub>60</sub>) was applied again. Finally, MTSEA-biotin (2 mM, 2 min) was applied alone, the cell was washed for 5 min, and the GABA (EC<sub>40</sub>-EC<sub>60</sub>) was applied to determine the full extent of the MTSEA-biotin reaction.

MTSEA-biotin was used because it is impermeable to the membrane, it is not charged, and its size (similar to SR-95531) is suitable for fitting within the binding site but is bulky enough to make it likely that covalently attaching it to an introduced cysteine will result in a functional effect. In addition, MTSEA-biotin was used to examine the accessibility of introduced cysteines in other regions of the GABA binding site (Boileau et al., 1999, 2002; Wagner and Czajkowski, 2001; Holden and Czajkowski, 2002; Newell and Czajkowski, 2003; Newell et al., 2004).

**Rate of MTSEA-Biotin Modification of Introduced Cysteines.** The rate of MTSEA-biotin covalent modification of accessible introduced cysteines was determined by measuring the outcome of sequential applications of low-concentration MTSEA-biotin on

$I_{GABA}$ . The protocol was as follows: EC<sub>20</sub>-EC<sub>60</sub> GABA was applied for 5 s, the cell was washed for 30 s, MTSEA-biotin was applied for 5 to 20 s, the cell was washed for 2 to 2.5 min, and the procedure was repeated until  $I_{GABA}$  no longer changed, indicating that the reaction was complete. Before the rate of MTSEA-biotin modification was measured, GABA was applied every 3 min until  $I_{GABA}$  varied  $\leq 3\%$ , demonstrating that the observed changes in  $I_{GABA}$  after application of MTSEA-biotin were due to effects of the MTSEA-biotin.

For all rate experiments, the change in current amplitude was plotted versus cumulative time of MTSEA-biotin exposure. We assume that the concentration of MTSEA-biotin does not change significantly during the reaction; thus, we can determine a pseudo-first-order rate constant from the rate of change in  $I_{GABA}$ . Peak current at each time point was normalized to the peak current at  $t = 0$ , and a pseudo-first-order rate constant ( $k_1$ ) was determined by fitting the data with a single exponential decay or growth function:  $y = \text{span} \times e^{-kt} + \text{plateau}$ . Because the data are normalized to  $I_{GABA}$  at time 0,  $\text{span} = 1 - \text{plateau}$ . The second-order rate constant ( $k_2$ ) for MTSEA-biotin reaction was determined by dividing the calculated pseudo-first-order rate constant by the concentration of MTSEA-biotin used (Pascual and Karlin, 1998). To verify the accuracy of the calculated rate constants, rates were determined using at least two different concentrations of MTSEA-biotin for several mutants (data not shown).

The effect of ligand on the rate of MTSEA-biotin modification was tested by coapplying GABA (EC<sub>90</sub>-EC<sub>100</sub>), SR-95531 (IC<sub>50</sub>-IC<sub>95</sub>), pentobarbital (50  $\mu$ M for low concentration, or 500-1000  $\mu$ M for high concentration), and flurazepam (1-10  $\mu$ M) with MTSEA-biotin. We use low concentrations of MTEA-biotin for short times, which we established does not maximally alter  $I_{GABA}$  at the start of the experiment and we used high concentrations of ligand. Thus, we can determine how the presence of ligand alters the reaction rate, because the covalent reaction has not gone to completion. For these studies,  $I_{GABA}$  was stabilized before the rate of MTS reaction was measured as follows: apply GABA (EC<sub>20</sub>-EC<sub>60</sub>) for 5 s, wash for 30 s, apply GABA, SR-95531, pentobarbital, or flurazepam at high concentration for 5 to 20 s, wash 2 to 5 min, and repeat the procedure. Wash times were adjusted to ensure that currents obtained from test pulses of GABA (EC<sub>20</sub>-EC<sub>60</sub>) after exposure to high concentrations of GABA, pentobarbital or flurazepam were within 3% of the previous GABA (EC<sub>20</sub>-EC<sub>60</sub>) current peak. This ensured complete wash-out of drugs and recovery from desensitization.

**Statistical Analysis.** All data are from at least three different oocytes from at least two different frogs. Data analysis was carried out using nonlinear regression analysis included in the Prism software package (GraphPad Software, San Diego, CA). Statistical analysis was conducted using a one-way analysis of variance, followed by a post hoc Dunnett's test. Log (EC<sub>50</sub>) and ( $K_I$ ) values were used for statistical analyses.

**Structural Homology Modeling.** A model of the extracellular ligand binding domain (LBD) of the GABA<sub>A</sub> receptor was built based on the structure of the AChBP (Brejc et al., 2001). The crystal structure of the AChBP was downloaded from RCSB Protein Data Bank (code 1I9B) and loaded into Swiss Protein Data Bank Viewer (<http://ca.expasy.org/spdbv>). The rat  $\alpha_1$  mature protein sequence from Thr<sup>12</sup>-Ile<sup>227</sup>, the  $\beta_2$  protein sequence from Ser<sup>10</sup>-Leu<sup>218</sup>, and the  $\gamma_2$  protein sequence from Gly<sup>25</sup>-Arg<sup>231</sup> were aligned with the AChBP primary amino acid sequence as depicted in Cromer et al. (2002) and threaded onto the AChBP tertiary structure using the "Interactive Magic Fit" function of Swiss Protein Data Bank Viewer. The threaded subunits were imported into SYBYL (Tripos, Inc., St. Louis, MO) where energy minimization was carried out. SYBYL minimizations terminate when the number of iterations is reached or if the gradient change reaches 0.05 kcal/ $\text{\AA} \times \text{mol}$ . The first 100 iterations were carried out using Simplex minimization (Press et al., 1988) followed by 1000 iterations using the Powell conjugate gradient method (Powell, 1977). A GABA<sub>A</sub> receptor LBD ( $\beta$ : $\alpha$ : $\beta$ : $\alpha$ : $\gamma$  viewed counterclockwise from the synaptic cleft) was assembled by overlay-

ing the monomeric subunits on the AChBP scaffold, and the resulting structure was imported into SYBYL and energy-minimized. Neither water nor entropy factors were included during the minimizations. After the global energy minimization, Ramachandran plots,  $\chi$  plots, side-chain positions, and *cis*- and *trans*- bonds were all examined. The program PROCHECK (Laskowski et al., 1993) was run to examine structural features against the established database of protein parameters, most importantly the  $\phi/\psi$  torsions and side-chain conformations. Problems in the structure that were revealed by these evaluations were fixed manually, and energy minimizations were run again as needed. Regions with insertions were modeled by fitting structures from a loop database. Because the sequence identity of the AChBP and the GABA<sub>A</sub> receptor LBD is only 18%, caution must be used in interpreting the absolute positions of individual side-chain residues in the model. Docking of GABA and SR-95531 was performed using the Flo+ version of QXP (Quick eXPlore; McMartin and Bohacek, 1997). The ligands were manually placed into the  $\beta/\alpha$  GABA binding site interface, and the docking simulation was carried out using a Metropolis modified Monte-Carlo search procedure for 1000 cycles with nearby side chains flexible. The lowest energy poses are shown in Fig. 8, C and D, and were produced using PyMOL (DeLano Scientific, LLC, San Carlos, CA).

## Results

### Expression and Functional Characterization of Cysteine Mutant Receptors. Twenty residues in the Met<sup>113</sup>–

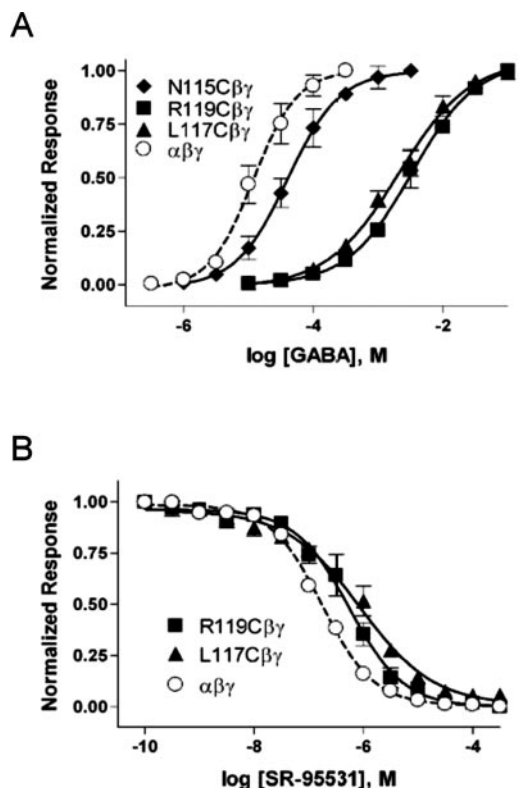


**Fig. 2.** GABA and SR-95531 concentration response curves for wild-type and mutant GABA<sub>A</sub> receptors. **A**, GABA concentration response curves for  $\alpha_1\beta_2\gamma_2$  (○),  $\alpha_1N115C\beta_2\gamma_2$  (◆),  $\alpha_1L117C\beta_2\gamma_2$  (▲), and  $\alpha_1R119C\beta_2\gamma_2$  (■) receptors expressed in *X. laevis* oocytes are shown. Data points were normalized to  $I_{max}$  and represent the mean  $\pm$  S.D. from at least three experiments. **B**, SR-95531 competition curves for  $\alpha_1\beta_2\gamma_2$  (○),  $\alpha_1L117C\beta_2\gamma_2$  (▲), and  $\alpha_1R119C\beta_2\gamma_2$  (■) receptors expressed in *X. laevis* oocytes are shown. Data points were normalized to  $I_{GABA}$  in the absence of blocker and represent the mean  $\pm$  S.D. from at least three experiments. All data were fit by nonlinear regression as described under *Materials and Methods*. GABA EC<sub>50</sub> and SR-95531 apparent  $K_I$  values are summarized in Table 1.

Leu<sup>132</sup> region of the GABA<sub>A</sub> receptor  $\alpha_1$  subunit were individually mutated to cysteine (Fig. 1) and expressed with wild-type  $\beta_2$  and  $\gamma_2$  subunits in *X. laevis* oocytes. All mutant subunits formed GABA-activated channels. Maximal GABA current amplitudes ranged from 1 to 10  $\mu$ A and did not differ significantly from maximal currents elicited from oocytes expressing wild-type  $\alpha_1\beta_2\gamma_2$  receptors, except for  $\alpha_1R119C\beta_2\gamma_2$  (see *Materials and Methods*).

GABA activated wild-type receptors with an EC<sub>50</sub> value of 13.1  $\mu$ M (Fig. 2, Table 1), and cysteine substitutions at  $\alpha_1Met^{113}$ ,  $\alpha_1Asn^{115}$ ,  $\alpha_1Lys^{116}$ ,  $\alpha_1Thr^{121}$ ,  $\alpha_1Thr^{125}$ , and  $\alpha_1Leu^{126}$  did not alter GABA sensitivity. Fourteen cysteine mutations significantly altered GABA EC<sub>50</sub> values compared with wild-type receptors (Table 1). The largest increases in GABA EC<sub>50</sub> values were observed for receptors containing  $\alpha_1R119C$ ,  $\alpha_1L117C$ , and  $\alpha_1T129C$  (261-, 161-, and 102-fold, respectively). Mutations of  $\alpha_1Arg^{131}$ ,  $\alpha_1Glu^{124}$ ,  $\alpha_1Tyr^{128}$ , and  $\alpha_1Leu^{118}$ , increased GABA EC<sub>50</sub> values 67-, 42-, 28-, and 25-fold, respectively, and cysteine substitutions of seven other residues ( $\alpha_1Pro^{114}$ ,  $\alpha_1Ile^{120}$ ,  $\alpha_1Glu^{122}$ ,  $\alpha_1Asp^{123}$ ,  $\alpha_1Leu^{127}$ ,  $\alpha_1Met^{130}$ , and  $\alpha_1Leu^{132}$ ) increased GABA EC<sub>50</sub> values by less than 15-fold. Seven cysteine substitutions,  $\alpha_1P114C$ ,  $\alpha_1L117C$ ,  $\alpha_1R119C$ ,  $\alpha_1T121C$ ,  $\alpha_1G124C$ ,  $\alpha_1Y128C$ , and  $\alpha_1R131C$ , significantly altered the sensitivity for the competitive antagonist SR-95531, and these changes were  $\leq$ 11-fold (Fig. 2, Table 1). The cysteine mutations had no effects on pentobarbital (50  $\mu$ M) or flurazepam (1–10  $\mu$ M) potentiation of GABA responses and no effects on the ability of pentobarbital (500  $\mu$ M–1 mM) to activate the receptor compared with wild-type receptors, suggesting that the global structure and function of the receptor was not altered by the cysteine mutations. Nonetheless, as in any mutagenesis study, one must keep in mind that the structure of the mutant receptor may not be the same as the structure of the wild-type receptor.

**TABLE 1**

GABA EC<sub>50</sub> values and SR-95531 apparent  $K_I$  values for introduced cysteines in the loop E region of the GABA<sub>A</sub> receptor

GABA EC<sub>50</sub> values and SR-95531 apparent  $K_I$  values were measured using two-electrode voltage clamp as described under *Materials and Methods*. All EC<sub>50</sub> and apparent  $K_I$  values are expressed as the average of at least three independent experiments  $\pm$  S.D.

Receptor	EC <sub>50</sub>	n	mut/wt	K <sub>I</sub>	n	mut/wt
	$\mu$ M			nM		
$\alpha_1\beta_2\gamma_2$	13.1 $\pm$ 3.7	4	1	110 $\pm$ 24	4	1
$\alpha_1M113C\beta_2\gamma_2$	18.4 $\pm$ 8.3	4	1.4	89.5 $\pm$ 5.5	3	0.8
$\alpha_1P114C\beta_2\gamma_2$	70.8 $\pm$ 20.5	4	5.4**	355.0 $\pm$ 67.4	3	3.2*
$\alpha_1N115C\beta_2\gamma_2$	41.6 $\pm$ 10.4	3	3.2	92.5 $\pm$ 16.4	3	0.8
$\alpha_1K116C\beta_2\gamma_2$	18.9 $\pm$ 12.0	4	1.4	92.0 $\pm$ 21.7	3	0.8
$\alpha_1L117C\beta_2\gamma_2$	2100 $\pm$ 272	5	160.6**	385 $\pm$ 256	3	3.5*
$\alpha_1L118C\beta_2\gamma_2$	320 $\pm$ 93.5	3	24.5**	83.7 $\pm$ 17.5	3	0.8
$\alpha_1R119C\beta_2\gamma_2$	3400 $\pm$ 910	3	260.5**	450 $\pm$ 135	3	4.0**
$\alpha_1I120C\beta_2\gamma_2$	170 $\pm$ 61	3	13.1**	170 $\pm$ 100	3	1.6
$\alpha_1T121C\beta_2\gamma_2$	11.5 $\pm$ 1.4	3	0.9	51.5 $\pm$ 5.0	3	0.5*
$\alpha_1E122C\beta_2\gamma_2$	36.2 $\pm$ 11.5	6	2.8	63.3 $\pm$ 13.1	3	0.6
$\alpha_1D123C\beta_2\gamma_2$	69.1 $\pm$ 24.5	3	5.3**	155 $\pm$ 17.5	3	1.4
$\alpha_1G124C\beta_2\gamma_2$	550 $\pm$ 120	3	42**	1155 $\pm$ 245	3	10.4**
$\alpha_1T125C\beta_2\gamma_2$	28.0 $\pm$ 5.6	3	2.1	85.7 $\pm$ 11.7	3	0.8
$\alpha_1L126C\beta_2\gamma_2$	49.3 $\pm$ 11.6	5	3.8*	101 $\pm$ 1.26	3	0.9
$\alpha_1L127C\beta_2\gamma_2$	190 $\pm$ 18	3	14.5**	167 $\pm$ 57	4	1.5
$\alpha_1Y128C\beta_2\gamma_2$	372 $\pm$ 31	3	28.4**	737 $\pm$ 99	3	6.7**
$\alpha_1T129C\beta_2\gamma_2$	1330 $\pm$ 329	8	102**	235 $\pm$ 102	3	2.1
$\alpha_1M130C\beta_2\gamma_2$	86.2 $\pm$ 25.8	5	6.6**	70.7 $\pm$ 2.8	3	0.64
$\alpha_1R131C\beta_2\gamma_2$	883 $\pm$ 358	6	67.4**	937 $\pm$ 279	3	8.5**
$\alpha_1L132C\beta_2\gamma_2$	86 $\pm$ 33.5	4	6.6**	299 $\pm$ 56	3	2.7

\* EC<sub>50</sub> and  $K_I$  values were statistically significant from wild type,  $P < 0.05$ .

\*\* EC<sub>50</sub> and  $K_I$  values were statistically significant from wild type,  $P < 0.01$ .

**Modification of Cysteine Mutants by MTSEA-Biotin.**

Reaction of wild-type  $\alpha_1\beta_2\gamma_2$  GABA<sub>A</sub> receptors with the sulfhydryl-specific reagent MTSEA-biotin (2 mM, 2 min) had no significant effect on GABA-mediated current amplitude ( $I_{GABA}$ ) (Fig. 3). MTSEA-biotin treatment significantly altered  $I_{GABA}$  in nine of the twenty mutant receptors (Fig. 3). In receptors containing  $\alpha_1$ M113C,  $\alpha_1$ N115C,  $\alpha_1$ K116C,  $\alpha_1$ L117C,  $\alpha_1$ R119C,  $\alpha_1$ T129C, and  $\alpha_1$ R131C, MTSEA-biotin inhibited  $I_{GABA}$  by 25, 27, 58, 81, 34, 60, and 76%, respectively. The observed decreases in  $I_{GABA}$  after MTS modification can result from the binding sites being physically blocked by the MTS reagent or from an increase in GABA  $EC_{50}$  and/or a decrease in maximal GABA response ( $I_{max}$ ) that arise from changes in GABA binding and/or channel gating. In receptors containing  $\alpha_1$ E122C and  $\alpha_1$ L127C, MTSEA-biotin potentiated  $I_{GABA}$  by 50 and 67%, respectively. We hypothesized that these observed increases in  $I_{GABA}$  were due to decreases in the GABA  $EC_{50}$  values of  $\alpha_1$ E122C $\beta_2\gamma_2$  and  $\alpha_1$ L127C $\beta_2\gamma_2$  receptors after MTSEA-biotin modification. To test this hypothesis, we measured GABA concentration responses in the same oocyte expressing  $\alpha_1$ E122C $\beta_2\gamma_2$  receptors before and after MTSEA-biotin ap-

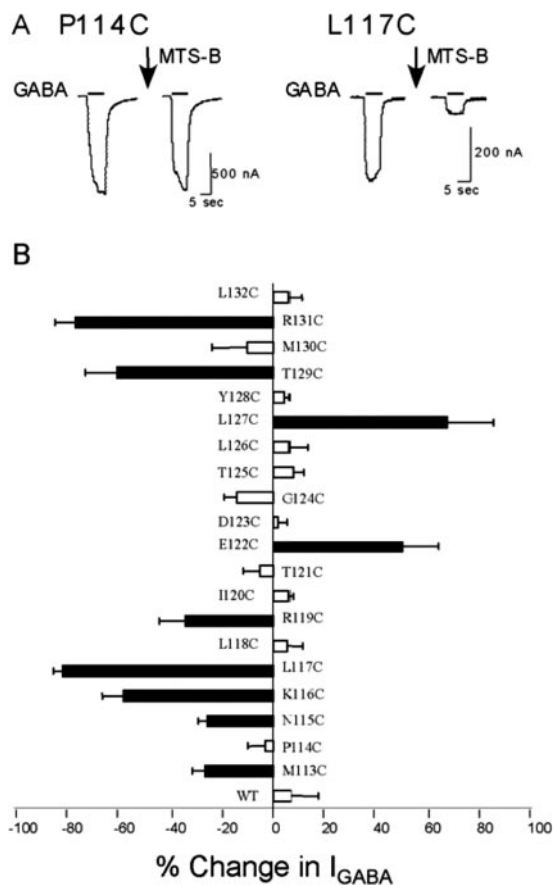


**Fig. 3.** Effects of MTSEA-biotin on GABA-evoked current recorded from oocytes expressing wild-type and mutant receptors. A, representative current traces recorded during application of GABA ( $EC_{40-60}$ ) before and after treatment with MTSEA-biotin (MTS-B, 2 mM, 2 min) from oocytes expressing  $\alpha_1$ P114C $\beta_2\gamma_2$  and  $\alpha_1$ L117C $\beta_2\gamma_2$  receptors. B, summary of the percentage inhibition or potentiation of current [percentage change =  $((I_{GABA, after} / I_{GABA, before}) - 1) \times 100$ ] resulting from MTSEA-biotin treatment of wild-type  $\alpha_1\beta_2\gamma_2$  receptors ( $\alpha\beta\gamma$ ) and mutant receptors is shown. Bars represent the mean  $\pm$  S.D. of at least three experiments. Black bars indicate that the percentage change is significantly different from wild type ( $p < 0.001$ ).

plication (Fig. 4). MTSEA-biotin modification of  $\alpha_1$ E122C-containing receptors resulted in an approximately 1.8-fold increase in GABA sensitivity, with no change in the maximal amount of current elicited by GABA. MTSEA-biotin had no effect on receptors containing  $\alpha_1$ P114C,  $\alpha_1$ L118C,  $\alpha_1$ I120C,  $\alpha_1$ T121C,  $\alpha_1$ D123C,  $\alpha_1$ G124C,  $\alpha_1$ T125C,  $\alpha_1$ L126C,  $\alpha_1$ Y128C,  $\alpha_1$ M130C, or  $\alpha_1$ L132C (Fig. 3). Thus, either these introduced cysteines were not accessible to MTSEA-biotin modification or their modification had no functional effect. The accessibility pattern of the residues is consistent with the predicted side-chain positions observed in homology models of the GABA<sub>A</sub> receptor, which depict this region of the receptor as forming  $\beta_5$ -loop- $\beta_5'$ -loop- $\beta_6$  (Fig. 1), and suggests that the positions of the introduced cysteines are similar to the wild-type residues.

**MTSEA-Biotin Rates of Reaction.** The rate at which MTSEA-biotin covalently modifies an accessible introduced cysteine depends on several factors, including the ionization of the sulfhydryl group, local steric restrictions, the electrostatic potential near the cysteine, and the permeability of the access pathway. Methanethiosulfonate reagents react  $10^9$  to  $10^{10}$  times faster with the ionized thiolate ( $RS^-$ ) form of cysteine than they do with the protonated form, and ionization is more likely in an aqueous environment (Roberts et al., 1986; Stauffer and Karlin, 1994). Thus, a cysteine in an open, aqueous environment will have a faster rate of reaction than a cysteine in a restrictive, nonpolar environment.

We measured the second-order rate constants for MTSEA-biotin modification of accessible introduced cysteines in the absence of ligands to establish rates of modification in the

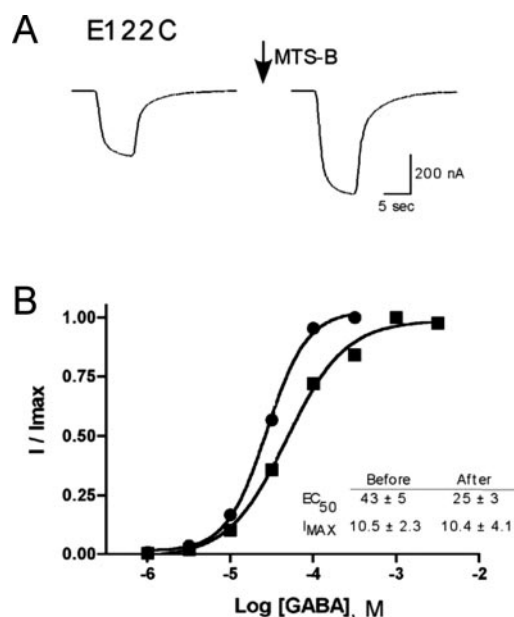


**Fig. 4.** MTSEA-biotin modification of E122C causes a potentiation of  $I_{GABA}$  and a leftward shift in the GABA dose-response curve. A, representative GABA ( $EC_{40-60}$ ) current traces recorded before and after treatment with MTSEA-biotin (MTS-B, 2 mM, 2 min) from an oocyte expressing  $\alpha_1$ E122C $\beta_2\gamma_2$  receptors demonstrating that current is increased after MTSEA-biotin application. B, GABA concentration response curves obtained from the same oocyte expressing  $\alpha_1$ E122C $\beta_2\gamma_2$  receptors before (■) and after (●) application of 2 mM MTSEA-biotin for 2 min. The GABA  $EC_{50}$  value is shifted leftward approximately 1.75-fold after application of MTSEA-biotin. The inserted table shows the mean GABA  $EC_{50}$  values (micromolar) and maximum  $I_{GABA}$  values (microamperes)  $\pm$  S.D. from three different oocytes.

TABLE 2

Rates of MTSEA-biotin covalent modification of accessible introduced cysteines in the loop E region of the GABA<sub>A</sub> receptor in the absence and presence of GABA, SR-95531, pentobarbital (PB) at low and high concentrations, and flurazepam (FLRZPM)

Rates of MTSEA-biotin reaction with accessible introduced cysteines were measured, and second-order rate constants ( $k_2$ ) were calculated as described under *Materials and Methods*. Second-order rate constants in this table reflect the means  $\pm$  S.D. ( $n$ ). Rates of modification of  $\alpha_1$ R119C were measured when expressed with wild-type  $\beta_2$  or wild-type  $\beta_3$  +  $\gamma_2$  subunits to determine whether the absence of the  $\gamma_2$  subunit would affect the rate and because high receptor expression levels were achieved in the absence of the  $\gamma_2$  subunit making the rates easier to measure. In addition, preliminary data indicates that the rate of modification of E122C in the presence of 50  $\mu$ M pentobarbital is 1.5-fold slower.

Receptor	$k_2$					
	Control	GABA	SR-95531	PB Low	PB High	FLRZPM
$\alpha_1$ K116C $\beta_2$	223 $\pm$ 53 (7)	73 $\pm$ 19 (3)**	246 $\pm$ 39 (5)	N.D.	258 $\pm$ 107 (5)	322 $\pm$ 128 (5)
$\alpha_1$ L117C $\beta_2$	151,000 $\pm$ 47,000 (6)	800 $\pm$ 80 (3)**	13,200 $\pm$ 3800 (3)**	N.D.	188,000 $\pm$ 98,000 (3)	159,000 $\pm$ 27,000 (3)
$\alpha_1$ R119C $\beta_2$	1170 $\pm$ 190 (3)	1100 $\pm$ 600 (3)	182 $\pm$ 67 (3)**	N.D.	N.D.	N.D.
$\alpha_1$ R119C $\beta_3$	1375 $\pm$ 362 (4)	1445 $\pm$ 338 (4)	172 $\pm$ 29 (4)**	N.D.	1120 $\pm$ 202 (3)	N.D.
$\alpha_1$ E122C $\beta_2$	14,200 $\pm$ 4500 (5)	5000 $\pm$ 2100 (4)**	11,300 $\pm$ 3700 (5)	N.D.	6600 $\pm$ 1500 (3)*	8100 $\pm$ 2500 (4)*
$\alpha_1$ L127C $\beta_2$	196,800 $\pm$ 62,200 (8)	54,960 $\pm$ 25,980 (3)**	29,850 $\pm$ 9460 (3)**	249,500 $\pm$ 31,500 (3)	288,100 $\pm$ 25,660 (3)	306,200 $\pm$ 54,100 (3)*
$\alpha_1$ T129C $\beta_2$	2,520,000 $\pm$ 472,000 (6)	33,970 $\pm$ 2600 (3)**	438,100 $\pm$ 147,900 (3)**	2,764,000 $\pm$ 475,500 (3)	1,643,000 $\pm$ 725,300 (3)	1,938,000 $\pm$ 493,400 (3)
$\alpha_1$ R131C $\beta_2$	400 $\pm$ 75 (5)	10.8 $\pm$ 8.0 (3)**	191 $\pm$ 106 (3)**	689 $\pm$ 120 (3)**	1650 $\pm$ 230 (3)**	800 $\pm$ 130 (3)**

N.D., not determined.

\* Rates of reaction in the presence of ligand that were statistically significant from control where  $P < 0.05$ .

\*\* Rates of reaction in the presence of ligand that were statistically significant from control where  $P < 0.01$ .

resting, closed state of the receptor. The fastest rates of covalent modification occurred at  $\alpha_1$ T129C,  $\alpha_1$ L127C,  $\alpha_1$ L117C, and  $\alpha_1$ E122C ( $k_2 \sim 25.2, 1.968, 1.51, \text{ and } 0.142 \times 10^5 \text{ M}^{-1}\text{s}^{-1}$ , respectively; Table 2), indicating that these residues are ionized and located in an open, aqueous environment. Slower rates were measured for  $\alpha_1$ R119C,  $\alpha_1$ R131C, and  $\alpha_1$ K116C ( $k_2 \sim 1170, 400, \text{ and } 223 \text{ M}^{-1}\text{s}^{-1}$ , respectively), suggesting that the thiol groups introduced at these positions are not as well ionized and/or the residues are located in a more restricted, buried environment. Although the rates measured are consistent with the predicted positions of these residues in a homology model of the extracellular ligand binding domain of the GABA<sub>A</sub> receptor, with  $\alpha_1$ Thr<sup>129</sup>,  $\alpha_1$ Leu<sup>127</sup>,  $\alpha_1$ Leu<sup>117</sup>, and  $\alpha_1$ Glu<sup>122</sup> being located in relatively accessible regions and  $\alpha_1$ Arg<sup>131</sup> and  $\alpha_1$ Lys<sup>116</sup> more buried (Fig. 8), the rates also depend on the local electrostatic potentials near the sulfhydryl groups, which are probably different at each position and contribute to the range of reaction rates measured. Rates of modification of  $\alpha_1$ M113C and  $\alpha_1$ N115C were not measured because of the small effect MTSEA-biotin modification had on  $I_{\text{GABA}}$  for these residues (<30%, Fig. 3).

**Effect of Orthosteric Ligands on MTSEA-Biotin Second-Order Rate Constants.** Orthosteric ligands bind to the GABA<sub>A</sub> receptor in the neurotransmitter binding site. To identify core binding site residues and to detect whether movements occur in and near the  $\alpha_1$ Met<sup>113</sup>-Leu<sup>132</sup> region during occupation of the binding site with orthosteric ligands, we measured the rates of modification of K116C, L117C, R119C, E122C, L127C, T129C, and R131C in the presence of the agonist GABA and the antagonist SR-95531. Changes in the rates of modification during orthosteric ligand binding can be due to steric block from the ligand itself or to local structural movements triggered by ligand binding.

In the presence of GABA ( $\sim \text{EC}_{90}$ ), the rates of modification of K116C, L117C, E122C, L127C, T129C, and R131C were significantly slowed by 3-, 200-, 3-, 40-, 74-, and 36-fold, respectively (Fig. 5, A and B; Table 2). In the presence of SR-95531 ( $\sim \text{EC}_{90}$ ), the rates of modification of L117C, R119C, L127C, T129C, and R131C were slowed 11-, 6-, 7-, 6-, and 2-fold, respectively (Fig. 5, A and B; Table 2).

Because MTSEA-biotin elicited only a small change in  $I_{\text{GABA}}$  for residues M113C and N115C (<30%; Fig. 3), we examined the effect of GABA and SR-95531 on the extent of inhibition of  $I_{\text{GABA}}$  induced by MTSEA-biotin modification. For M113C, only GABA decreased MTSEA-biotin inhibition of  $I_{\text{GABA}}$ , whereas both GABA and SR-95531 decreased MTSEA-biotin inhibition of  $I_{\text{GABA}}$  for N115C (Fig. 5, C and D). In summary, both GABA and SR-95531 decreased modification of five introduced cysteines: N115C, L117C, L127C, T129C, and R131C. For three mutants, M113C, K116C, and E122C, only GABA slowed their modification, whereas modification of R119C was slowed only by SR-95531.

**Effect of Pentobarbital on MTSEA-Biotin Second-Order Rate Constants.** To identify conformational changes that occur within or near the  $\alpha_1$ Met<sup>113</sup>-Leu<sup>132</sup> region during channel gating, we measured the rate of modification of accessible introduced cysteine residues in the presence of pentobarbital. Pentobarbital binds to a site that is distinct from the neurotransmitter binding pocket (Amin and Weiss, 1993) and, at high concentrations, directly activates the GABA<sub>A</sub> receptor. Thus, pentobarbital is a useful tool for monitoring

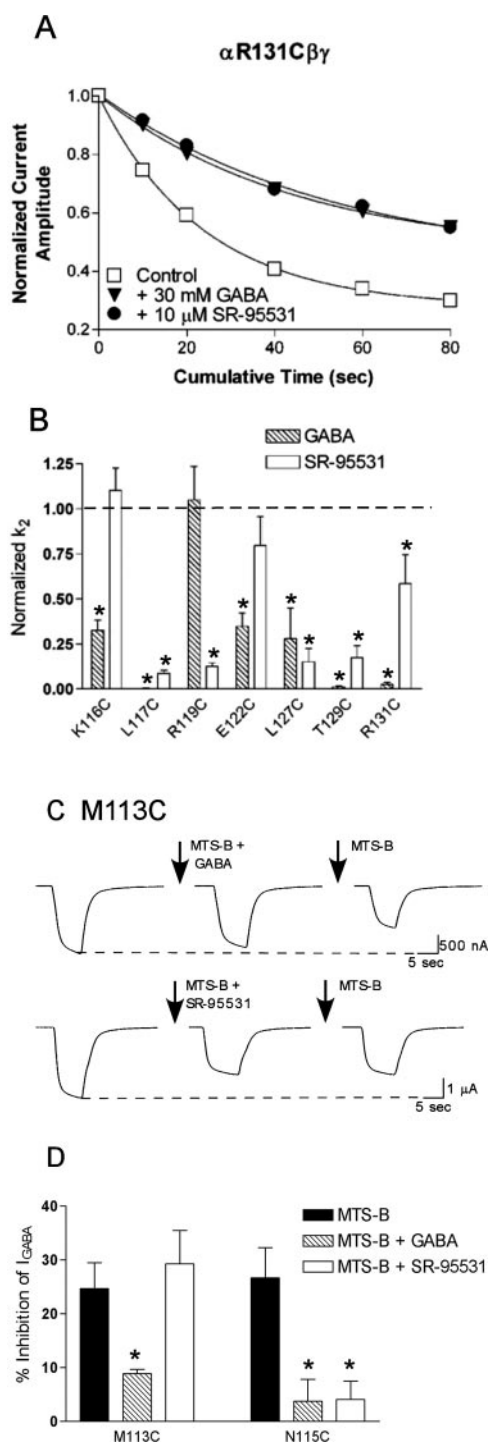


**Fig. 5.** Effects of orthosteric ligands on MTSEA-biotin modification of introduced cysteine residues. **A**, representative single exponential curve fits from individual experiments measuring the rate of modification of  $\alpha_1$ R131C with MTSEA-biotin alone (□), MTSEA-biotin + GABA (▼), and MTSEA-biotin + SR-95531 (●). Rate experiments were performed as described under *Materials and Methods*. Decreases in  $I_{GABA}$  were plotted versus cumulative time of MTSEA-biotin exposure. Data were normalized to the current measured at  $t = 0$  for each experiment. **B**, summary of the effect of GABA and SR-95531 on the rate at which MTSEA-biotin modifies the introduced cysteines. Second-order rate constants were calculated in the presence of GABA and SR-95531 as described under *Materials and Methods* and, for each mutant, were normalized to the control rate (MTSEA-biotin alone, dashed line). Data represent the mean  $\pm$  S.D. for at least three experiments, and \* indicates that the rate is significantly different from control rate,  $p < 0.01$ . **C**, GABA-induced current traces from oocytes expressing  $\alpha_1$ M113C $\beta_2\gamma_2$  receptors before and

conformational movements that occur within or near the GABA binding site during channel gating without sterically blocking the GABA binding pocket.

The rates of modification of most of the introduced cysteines were not altered in the presence of a concentration of pentobarbital that activates the receptor (500–1000  $\mu$ M) (K116C, L117C, R119C, L127C, and T129C; Fig. 6 and Table 2). However, pentobarbital (500  $\mu$ M) significantly decreased the rate of modification of E122C by  $\sim$ 2-fold and significantly increased modification of R131C by  $\sim$ 4-fold (Fig. 6D, Table 2). It is noteworthy that concentrations of pentobarbital that do not open the channel but potentiate GABA current ( $\sim$ 50  $\mu$ M) increased the rate of modification of R131C by  $\sim$ 2-fold (Table 2).

**Effect of Flurazepam on MTSEA-Biotin Second-Order Rate Constants.** BZDs, used clinically for their anxiolytic and sedative actions, allosterically modulate GABA<sub>A</sub> receptor current responses. The structural mechanisms underlying how BZDs alter GABA-activation of the receptor are not well known. To identify whether local conformational movements occur within or near the GABA binding site during allosteric modulation of the GABA<sub>A</sub> receptor by a BZD, we measured the rates of modification of accessible introduced cysteines in the presence of the BZD-positive allosteric modulator flurazepam.

Flurazepam ( $\sim$ EC<sub>90</sub>) increased the rates of MTSEA-biotin modification of L127C and R131C by approximately 2-fold, whereas it decreased the rate of modification of E122C by approximately 2-fold (Fig. 7, Table 2). Flurazepam had no effect on the rates of modification of K116C, L117C, and T129C (Table 2). The ability of flurazepam to alter the rates of modification of E122C, L127C, and R131C demonstrates that residues in the  $\beta$ : $\alpha$  binding site interface undergo structural rearrangements during occupation of the BZD binding site.

## Discussion

Protein movements underlying LGIC activation and allosteric drug modulation are not well established. Here, we used the substituted cysteine accessibility method to examine the dynamics of the  $\alpha_1$ Met<sup>113</sup>-Leu<sup>132</sup> region of the GABA<sub>A</sub> receptor agonist binding site (loop E) and determined that orthosteric ligand binding, channel gating, and allosteric drug modulator binding each induce distinct structural rearrangements in this region.

**GABA Binding Site Residues.** Residues that line the GABA binding site may directly contact ligand, be important for maintaining binding site structure, and/or mediate local conformational movements important for activation and/or desensitization. We identified four residues,  $\alpha_1$ Asn<sup>115</sup>,

after a 2-min coapplication of 2 mM MTSEA-biotin (MTS-B) + EC<sub>95</sub> GABA (top) or 2 mM MTSEA-biotin + EC<sub>90</sub> SR-95531 (bottom), and then after application of MTSEA-biotin alone, demonstrating that only GABA protects  $\alpha_1$ M113C from covalent modification. The dotted lines represent the peak amplitude of current elicited by EC<sub>50</sub> GABA before MTSEA-biotin application. **D**, summary of the percentage inhibition of current [percentage change =  $((I_{GABA, after} / I_{GABA, before}) - 1) \times 100$ ] resulting from MTSEA-biotin treatment of  $\alpha_1$ M113C $\beta_2\gamma_2$  receptors and  $\alpha_1$ N115C $\beta_2\gamma_2$  receptors in the presence and absence of GABA and SR-95531. Bars represent the mean  $\pm$  S.D. from at least three experiments. \*, values that are significantly different ( $p < 0.001$ ) from inhibition by MTSEA-biotin alone.

$\alpha_1\text{Leu}^{117}$ ,  $\alpha_1\text{Thr}^{129}$ , and  $\alpha_1\text{Arg}^{131}$ , that line the GABA binding pocket. When mutated to cysteine, these residues were modified by MTSEA-biotin, which decreased  $I_{\text{GABA}}$ . The rates or extents of modification were decreased in the presence of GABA and SR-95531. Pentobarbital-mediated activation did not slow MTSEA-biotin modification of L117C, T129C, and R131C, suggesting that GABA slowed their modification because of steric block rather than global channel-gating phenomenon. When mapped onto our homology model, these residues form part of the back wall of the binding pocket and face into the site (Fig. 8A). Detailed kinetic analyses are required to quantitatively determine the mutations' effects on microscopic binding affinity and channel gating kinetics. Recently, Sedelnikova et al. (2005) determined that residues in positions aligned to  $\alpha_1\text{Leu}^{117}$ ,  $\alpha_1\text{Thr}^{129}$ , and  $\alpha_1\text{Arg}^{131}$  line the GABA<sub>C</sub> receptor binding site.

In our structure,  $\alpha_1\text{Leu}^{117}$  lines the back wall of the binding pocket and faces into the site behind  $\alpha_1\text{Thr}^{129}$ . Based on our dockings,  $\alpha_1\text{Leu}^{117}$  is unlikely to be involved in contacting GABA or SR-95531 but possibly contributes to maintaining the site's structure via a hydrophobic interaction with  $\beta_2\text{Tyr}^{157}$ . The  $C_\beta$  atom of  $\alpha_1\text{Leu}^{117}$  is less than 6 Å from the  $C_\beta$  atom of  $\beta_2\text{Tyr}^{157}$ , a residue that forms part of the binding site's aromatic box.  $\alpha_1\text{Arg}^{131}$ , which also lines the back wall of the pocket, may maintain binding site structure via a salt-bridge interaction with  $\beta_2\text{Asp}^{101}$  (Harrison and Lummiss, 2006) or could be part of a trio of arginines ( $\alpha_1\text{Arg}^{66}$ ,

$\alpha_1\text{Arg}^{131}$ ,  $\beta_2\text{Arg}^{207}$ ) proposed to stabilize GABA's negatively charged carboxylate (Holden and Czajkowski, 2002; Wagner et al., 2004).

**Orthosteric Ligand-Mediated Movements.** As with the GABA<sub>A</sub> receptor  $\alpha_1$  subunit loop D region (Holden and Czajkowski, 2002), we have identified residues in the loop E region that change accessibility in response to only GABA or SR-95531. GABA decreased modification of M113C, K116C, and E122C, whereas SR-95531 decreased modification of R119C (Fig. 5D, Table 2). Decreases in modification can result from ligand physically blocking access to the cysteine or to movements induced by ligand binding. Because  $\alpha_1\text{Glu}^{122}$  is located far from the binding pocket (Fig. 8B), the change in E122C accessibility as a result of GABA probably reflects movements associated with GABA-induced channel gating. Consistent with this idea, activating concentrations of pentobarbital also decreased E122C accessibility, whereas SR-95531, which does not open the channel, had no effect. In addition, GABA application changed fluorescence of a label attached to E122C (and the aligned GABA<sub>C</sub> receptor residue) simultaneously with channel opening (Chang and Weiss, 2002; Muroi et al., 2006) providing evidence that  $\alpha_1\text{Glu}^{122}$  and/or nearby residues move in response to channel activation.

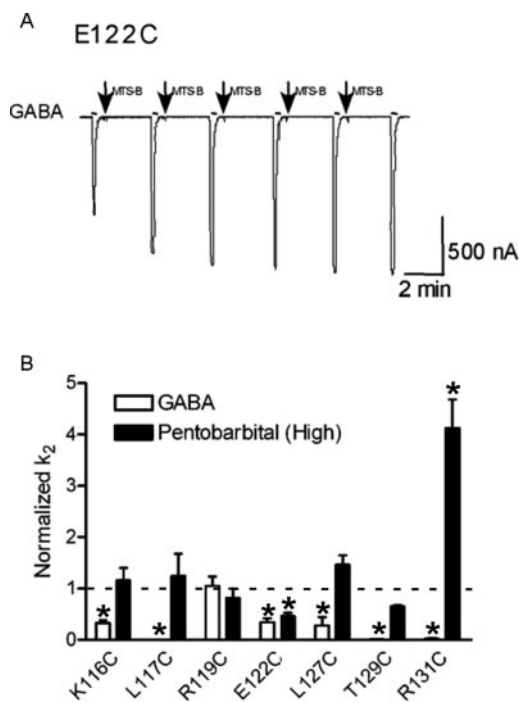


**Fig. 6.** Effects of pentobarbital on the rates of MTSEA-biotin modification of introduced cysteine residues. A, representative current traces depicting the effects of successive applications of MTSEA-biotin (MTS-B, arrows) on current elicited by GABA ( $\sim\text{EC}_{25}$ ) in oocytes expressing  $\alpha_1\text{E122C}\beta_2\gamma_2$  receptors. B, summary of the effect of GABA and pentobarbital on the rate at which MTSEA-biotin modifies the introduced cysteines. Second-order rate constants were calculated in the presence of GABA and pentobarbital as described under *Materials and Methods* and, for each mutant, were normalized to the control rate (MTSEA-biotin alone, dashed line). Bars represent the mean  $\pm$  S.E.M. for at least three experiments, and \* indicates that the rate is significantly different from control rate,  $p < 0.05$ .

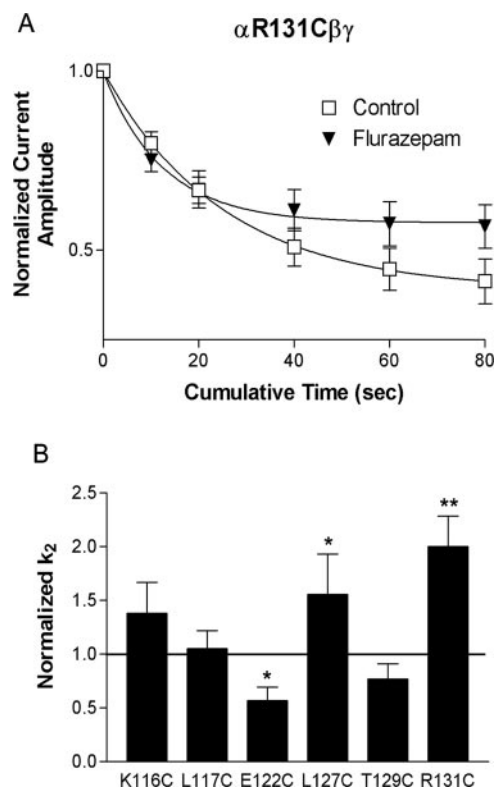


**Fig. 7.** Effect of flurazepam on rates of MTSEA-biotin modification of introduced cysteine residues. A, exponential curve fits from experiments measuring the rate of modification of  $\alpha_1\text{R131C}$  with MTSEA-biotin alone ( $\square$ ) and MTSEA-biotin + Flurazepam ( $\blacktriangledown$ ). Rate experiments were performed as described under *Materials and Methods*. Decreases in  $I_{\text{GABA}}$  were plotted versus cumulative time of MTSEA-biotin exposure. Data were normalized to the current measured at  $t = 0$  for each experiment. B, second-order rate constants were measured in the presence of flurazepam as described under *Materials and Methods* and, for each mutant, were normalized to the control rate (MTSEA-biotin alone, dashed line). Bars and data points represent the mean  $\pm$  S.D. for at least three experiments, and \* indicates that the rate is significantly different from control rate,  $p < 0.05$ ; \*\*,  $p < 0.01$ .

The decreases in modification of M113C and K116C by GABA and not by SR-95531 are more difficult to interpret because these residues are located near identified GABA

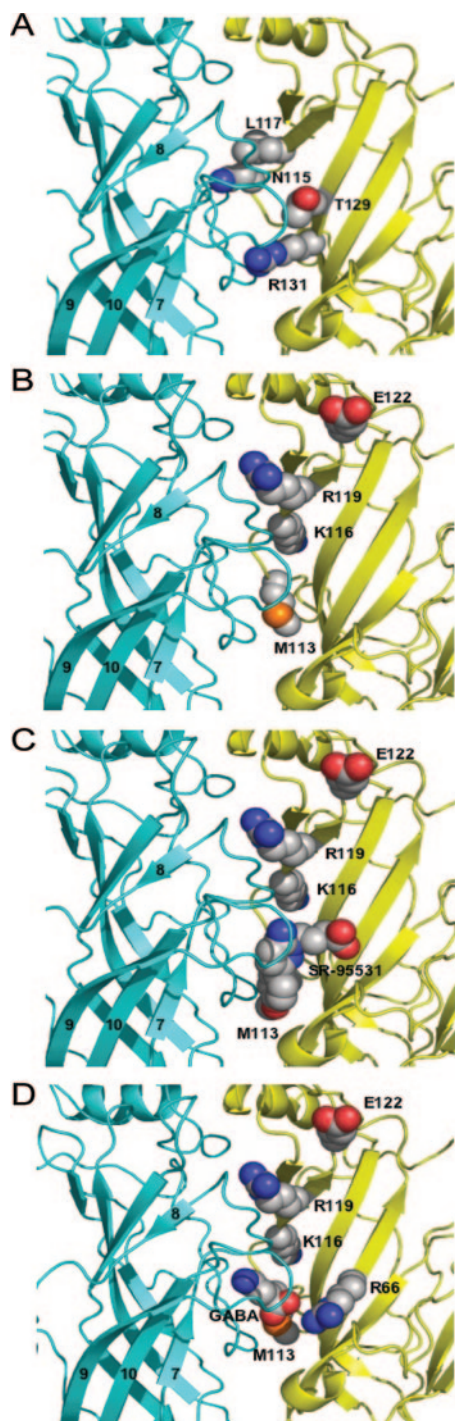


**Fig. 8.** Homology model of the extracellular N-terminal domains of the  $\beta$ - $\alpha$  subunit interface of the GABA<sub>A</sub> receptor. The  $\beta_2$  subunit is shown in cyan and the  $\alpha_1$  subunit in yellow.  $\beta$ -Strands 7, 8, 9, and 10 in the  $\beta_2$  subunit are numbered. A, residues in loop E that line the GABA binding site are space-filled. B, several residues that are conformationally sensitive to orthosteric ligand binding, channel gating or BZD modulation are space-filled. C, SR-95531 (space-filled) computationally docked into the GABA-binding site positions the positively charged end (red) facing the  $\alpha_1$  subunit near  $\alpha_1$ Arg<sup>66</sup> and the negatively charged end (blue) near  $\beta_2$ Tyr<sup>205</sup>. D, GABA (space-filled) computationally docked into the GABA-binding site positions the positively charged carboxylate near  $\alpha_1$ Arg<sup>66</sup> and the negatively charged amino group near  $\beta_2$ Tyr<sup>205</sup>.

binding site residues (Fig. 8B). Although we cannot rule out the possibility that decreases in their modification are due to physical block by GABA, this is unlikely. If the decreases were due to steric block, one would predict that both GABA and SR-95531 would decrease MTSEA-biotin modification of the residues, based on the larger size of SR-95531 (264 Å<sup>3</sup>) compared with GABA (99 Å<sup>3</sup>) and the overlapping positions of these ligands relative to  $\alpha_1$ Met<sup>113</sup> and  $\alpha_1$ Lys<sup>116</sup> when computationally docked into a homology model of the binding site (Fig. 8, C and D). Because SR-95531 had no effect on the rate of modification of M113C and K116C, the data suggest that these residues change accessibility due to local movements specifically triggered by GABA binding. Furthermore, in our homology model,  $\alpha_1$ Met<sup>113</sup> and  $\alpha_1$ Lys<sup>116</sup> are pointing away from the core of the GABA binding site.

Structural studies (Unwin et al., 2002; Celie et al., 2004) as well as molecular dynamic simulations (Law et al., 2005) in the nACh receptor and AChBP suggest that agonist binding promotes movement of loop C inward toward loop E to cap the binding site. We envision this capping motion to trap GABA within the site and block MTSEA-biotin from M113C and K116C. SR-95531, although considerably larger than GABA, is an antagonist and presumably does not promote this movement of loop C and thus does not change these residues accessibility. Furthermore, our data demonstrating that GABA decreased the rates of modification of the binding site residues L117C, T129C, and R131C (200-, 74-, and 36-fold, respectively) to a larger extent than SR-95531 (11-, 6-, and 2-fold, respectively) are also consistent with the idea that GABA binding stabilizes a conformation of the binding site that is more restrictive and less accessible than a SR-95531 bound site. Taken together, the data provide evidence that GABA binding promotes binding site closure.

After MTSEA-biotin modification of L127C, GABA-elicited currents are potentiated (Fig. 3), demonstrating that tethering ethyl-biotin onto L127C does not inhibit the ability of GABA to bind and trigger channel opening. Thus, L127C does not lie within the binding site and the decreases observed in the rate of modification of L127C by GABA and SR-95531 are a result of structural changes induced by their binding. Thus, although SR-95531 occupation of the GABA binding site does not trigger channel opening, it does cause local structural rearrangements. Movements triggered by competitive antagonist binding have been identified in glutamate (Armstrong and Gouaux, 2000), GABA<sub>A</sub> (Boileau et al., 2002; Muroi et al., 2006), and GABA<sub>C</sub> receptors (Chang and Weiss, 2002). It is noteworthy that SR-95531 decreased R119C modification, whereas GABA had no effect, suggesting that antagonist-induced movements are distinct from agonist-induced movements. Additional experiments are needed to confirm that the effects observed are due to the ligands' functional properties (i.e., agonist, antagonist) and not to differences in size or chemical property.

**Pentobarbital- versus GABA-Mediated Gating Movements.** Although GABA and pentobarbital binding probably stabilize comparable open-state structures because they produce similar single channel conductances (Jackson et al., 1982), some of the protein movements initially triggered by their binding must be different as they bind to distinct sites (Amin and Weiss, 1993). Thus, to examine global protein movements associated with channel gating as well as unique movements triggered by GABA and pentobarbital binding,

we measured MTSEA-biotin modification rates in the presence of an activating concentration of pentobarbital (500–1000  $\mu\text{M}$ ) and compared these with rates measured in the presence of GABA.

For E122C, both GABA and pentobarbital decreased the rate of MTSEA-biotin modification suggesting that, at least near Glu<sup>122</sup>, movements triggered by their binding are similar and that E122C reports gating-induced global movements. For R131C, pentobarbital significantly increased whereas GABA significantly decreased MTSEA-biotin modification. Arg<sup>131</sup> is located in the GABA binding site core; thus, the slowing of modification by GABA is probably due to steric block by GABA. Pentobarbital's increase in modification of R131C, however, demonstrates that this region of the GABA binding site, even when unoccupied by orthosteric ligand, undergoes movements in response to pentobarbital binding/channel activation. To date, we have identified 13 of 28 positions in the GABA binding site interface that change accessibility during pentobarbital binding/gating ( $\beta_2$ T160C,  $\beta_2$ D163C,  $\beta_2$ G203C,  $\beta_2$ S204C,  $\beta_2$ R207C,  $\beta_2$ S209C,  $\alpha_1$ D62C,  $\alpha_1$ S68C,  $\alpha_1$ E122C,  $\alpha_1$ R131C,  $\alpha_1$ V180C,  $\alpha_1$ A181C, and  $\alpha_1$ R186C; Wagner and Czajkowski 2001; Holden and Czajkowski 2002; Newell and Czajkowski, 2003; Newell et al., 2004). At several positions (K116C, L117C, L127C, and T129C) GABA decreased rates of modification whereas pentobarbital had no effect. As discussed above, the ability of GABA to alter L127C modification was probably due to GABA-induced local movements and not physical block. Thus, pentobarbital's lack of effect at this position suggests that L127C reports unique movements associated with GABA binding/activation of the receptor.

**Benzodiazepine-Mediated Movements.** BZD binding allosterically triggers movements in the  $\alpha_1$ Met<sup>113</sup>- $\alpha_1$ Leu<sup>132</sup> region of the GABA binding site. Flurazepam significantly altered the rate of E122C modification to a similar extent as GABA and pentobarbital, and increased modification of R131C similar to pentobarbital (Table 2). Thus, flurazepam binding triggered a subset of the same movements in the receptor that GABA and pentobarbital gating induced. Consistent with this hypothesis, recent experiments indicate that BZD positive modulators stabilize the receptor's open versus the closed state perturbing the receptor's gating equilibrium (Downing et al., 2005; Rusch and Forman, 2005; Campo-Soria et al., 2006).

Flurazepam binding also induces unique movements within the GABA binding site interface. Flurazepam increased the rate of L127C modification, whereas GABA decreased its rate and pentobarbital had no effect. Thus, each ligand can trigger different conformational changes in the  $\alpha_1$ Met<sup>113</sup>- $\alpha_1$ Leu<sup>132</sup> region. We speculate that these unique movements are the result of their binding to distinct sites and triggering different activation pathways that lead to their functional effects. Identifying these structural pathways is an important goal for future studies.

#### Acknowledgments

We thank Jill Smith for help in constructing the cysteine mutants, and Lisa Sharkey, Amy Kucken, Dr. Glen Newell, and James Seffinga-Clark for treating oocytes. In addition, we thank Dr. Ken Satyshur for help in constructing the models shown in this article and Dr. Glen Newell for critical reading of the manuscript.

#### References

- Akabas MA (2004) GABA<sub>A</sub> receptor structure-function studies: a reexamination in light of new acetylcholine receptor structures. *Int Rev Neurobiol* **62**:1–43.
- Amin J and Weiss DS (1993) GABA<sub>A</sub> receptor needs two homologous domains of the beta-subunit for activation by GABA but not by pentobarbital. *Nature (Lond)* **366**:565–569.
- Armstrong N and Gouaux E (2000) Mechanisms for activation and antagonism of an AMPA-sensitive glutamate receptor: crystal structures of the GlyR2 ligand binding core. *Neuron* **28**:165–181.
- Beene DL, Price KL, Lester HA, Dougherty DA, and Lummis SC (2004) Tyrosine residues that control binding and gating in the 5-hydroxytryptamine 3 receptor revealed by unnatural amino acid mutagenesis. *J Neurosci* **24**:9097–9104.
- Boileau AJ, Evers AR, Davis AF, and Czajkowski C (1999) Mapping the agonist binding site of the GABA<sub>A</sub> receptor: evidence for a beta-strand. *J Neurosci* **19**:4847–4854.
- Boileau AJ, Kucken AM, Evers AR, and Czajkowski C (1998) Molecular dissection of benzodiazepine binding and allosteric coupling using chimeric  $\gamma$ -aminobutyric acid A receptor subunits. *Mol Pharmacol* **53**:295–303.
- Boileau AJ, Newell JG, and Czajkowski C (2002) GABA(A) receptor beta 2 Tyr97 and Leu99 line the GABA-binding site. Insights into mechanisms of agonist and antagonist actions. *J Biol Chem* **277**:2931–2937.
- Brejck K, van Dijk WJ, Klaassen RV, Schuurmans M, van Der Oost J, Smit AB, and Sixma TK (2001) Crystal structure of an ACh-binding protein reveals the ligand-binding domain of nicotinic receptors. *Nature (Lond)* **411**:269–276.
- Campo-Soria C, Chang Y, and Weiss DS (2006) Mechanism of action of benzodiazepines on GABA<sub>A</sub> receptors. *Br J Pharmacol* **148**:984–990.
- Celie PH, van Rossum-Fikkert SE, van Dijk WJ, Brejck K, Smit AB, and Sixma TK (2004) Nicotine and carbamylcholine binding to nicotinic acetylcholine receptors as studied in AChBP crystal structures. *Neuron* **41**:907–914.
- Chang Y and Weiss DS (2002) Site-specific fluorescence reveals distinct structural changes with GABA activation and antagonism. *Nat Neurosci* **5**:1163–1168.
- Changeux JP and Edelstein SJ (1998) Allosteric receptors after 30 years. *Neuron* **21**:959–980.
- Cheng Y and Prusoff WH (1973) Relationship between the inhibition constant (KI) and the concentration of an inhibitor which causes 50 per cent inhibition (IC50) of an enzymatic reaction. *Biochem Pharmacol* **22**:3099–3108.
- Chou T (1974) Relationships between inhibition constants and fractional inhibition in enzyme-catalyzed reactions with different numbers of reactants, different reaction mechanisms, and different types of inhibition. *Mol Pharmacol* **10**:235–247.
- Cromer B, Morton CJ, and Parker MW (2002) Anxiety over GABA(A) receptor structure relieved by AChBP. *Trends Biochem Sci* **27**:280–287.
- Downing SS, Lee YT, Farb DH, and Gibbs TT (2005) Benzodiazepine modulation of partial agonist efficacy and spontaneously active GABA(A) receptors supports an allosteric model of modulation. *Br J Pharmacol* **145**:894–906.
- Harrison NJ and Lummis SCR (2006) Locating the carboxylate group of GABA in the homomeric rho GABA<sub>A</sub> receptor ligand-binding pocket. *J Biol Chem* **284**:24455–61.
- Holden JH and Czajkowski C (2002) Different residues in the GABA(A) receptor  $\alpha_1$ T60- $\alpha_1$ K70 region mediate GABA and SR-95531 actions. *J Biol Chem* **277**:18785–92.
- Jackson MB, Lecar H, Mathers DA, and Barker JL (1982) Single channel currents activated by gamma-aminobutyric acid, muscimol, and (-)-pentobarbital in cultured mouse spinal neurons. *J Neurosci* **2**:889–894.
- Kucken AM, Wagner DA, Ward PR, Teissere JA, Boileau AJ, and Czajkowski C (2000) Identification of benzodiazepine binding site residues in the  $\gamma_2$  subunit of the gamma-aminobutyric acid (A) receptor. *Mol Pharmacol* **57**:932–939.
- Laskowski RA, Moss DS, and Thornton JM (1993) Main chain bond lengths and bond angles in protein structures. *J Mol Biol* **231**:1049–1067.
- Law RJ, Henschman RH, and McCammon JA (2005) A gating mechanism proposed from a simulation of a human  $\alpha_7$  nicotinic acetylcholine receptor. *Proc Natl Acad Sci* **102**:6813–6818.
- McMartin C and Bohacek R (1997) QXP: Powerful, rapid computer algorithms for structure-based drug design. *J Comput Aided Mol Des* **11**:333–344.
- Muroi Y, Czajkowski C, and Jackson MB (2006) Local and global ligand-induced changes in the structure of the GABA<sub>A</sub> receptor. *Biochemistry* **45**:7013–7022.
- Newell JG and Czajkowski C (2003) The GABA<sub>A</sub> receptor  $\alpha_1$  subunit Pro176-Asp191 segment is involved in GABA binding and channel gating. *J Biol Chem* **278**:13166–13170.
- Newell JG, McDevitt RA, and Czajkowski C (2004) Mutation of glutamate 155 of the GABA<sub>A</sub> receptor beta2 subunit produces a spontaneously open channel: a trigger for channel activation. *J Neurosci* **24**:11226–35.
- Ohno K, Wang HL, Milone M, Bren N, Bregman JM, Nakano S, Quiram P, Pruitt JN, Sine SM, and Engel AG (1996) Congenital myasthenic syndrome caused by decreased agonist binding affinity due to a mutation in the acetylcholine receptor epsilon subunit. *Neuron* **17**:157–170.
- Pascual JM and Karlin A (1998) State dependent accessibility and electrostatic potential in the channel of the acetylcholine receptor. Inferences from rates of reaction of thiosulfonates with substituted cysteines in the M2 segment of the alpha subunit. *J Gen Physiol* **111**:717–739.
- Powell MJD (1977) Restart procedures for the conjugate gradient method. *Math Prog* **12**:241–254.
- Press WH, Flannery BP, Teukolsky SA, and Vetterling WT (1988) Conjugate gradients, simplex, and BFGS, in *Numerical Recipes in C: The Art of Scientific Computing*, pp 301–327. Cambridge University Press, Cambridge, UK.
- Roberts DD, Lewis SD, Ballou DP, Olson ST, and Shafer JA (1986) Reactivity of small thiolate anions and cysteine-25 in papain toward methyl methanethiosulfonate. *Biochemistry* **25**:5595–5601.
- Rusch D and Forman SA (2005) Classic benzodiazepines modulate the open-close equilibrium in alpha1beta2gamma2L gamma-aminobutyric acid type A receptors. *Anesthesiology* **102**:783–792.

- Sedelnikova A, Smith CD, Zakharkin SO, Weiss DS, and Chang Y (2005) Mapping the rho1 GABA-C receptor agonist binding pocket. Constructing a complete model. *J Biol Chem* **280**:1535–1542.
- Sieghart W and Sperk G (2002) Subunit composition, distribution, and function of GABA(A) receptor subtypes. *Curr Top Med Chem* **2**:795–816.
- Sigel E, Baur R, Kellenberger S, and Malherbe P (1992) Point mutations affecting antagonist affinity and agonist dependent gating of GABA<sub>A</sub> receptor channels. *EMBO (Eur Mol Biol Organ) J* **11**:2017–2023.
- Sigel E (2002) Mapping of the benzodiazepine recognition site on GABA(A) receptors. *Curr Top Med Chem* **2**:833–839.
- Smith GB and Olsen RW (1994) Identification of a [<sup>3</sup>H]muscimol photoaffinity substrate in the bovine  $\gamma$ -aminobutyric acid A receptor  $\alpha$  subunit. *J Biol Chem* **269**:20380–7.
- Stauffer DA and Karlin A (1994) Electrostatic potential of the acetylcholine binding sites in the nicotinic receptor probed by reactions of binding-site cysteines with charged methanethiosulfonates. *Biochemistry* **33**:6840–6849.
- Unwin N (2005) Refined structure of the nicotinic acetylcholine receptor at 4 Å resolution. *J Mol Biol* **346**:967–989.
- Unwin N, Miyazawa A, Li J, and Fujiyoshi Y (2002) Activation of the nicotinic acetylcholine receptor involves a switch in a conformation of the alpha subunits. *J Mol Biol* **319**:1165–1176.
- Venkataraman P, Venkatachalan SP, Joshi PR, Muthalagi M, and Schulte MK (2002) Identification of critical residues in loop E in the 5-HT<sub>3</sub>ASR binding site. *BMC Biochem* **3**:15.
- Wagner DA and Czajkowski C (2001) Structure and dynamics of the GABA binding pocket: A narrowing cleft that constricts during channel activation. *J Neurosci* **21**:67–74.
- Wagner DA, Czajkowski C, and Jones MV (2004) An arginine involved in GABA binding and unbinding but not gating of the GABA(A) receptor. *J Neurosci* **24**:2733–2741.
- Westh-Hansen SE, Witt MR, Dekermendjian K, Liljefors T, Rasmussen PB, and Nielsen M (1999) Arginine residue 120 of the human GABAA receptor alpha 1 subunit is essential for GABA binding and chloride ion current gating. *Neuroreport* **10**:2417–2421.

---

**Address correspondence to:** Dr. Cynthia Czajkowski, Department of Physiology, University of Wisconsin at Madison, 601 Science Drive, Madison, WI 53711. E-mail: czajkowski@physiology.wisc.edu

---